DESIGN CONCEPTS OF MODERN ACCELERATOR VACUUM SYSTEMS —PREDICTION VS. EXPERIMENTAL DATA*

Finn S. Reinath and D. T. Scalise

Lawrence Radiation Laboratory
University of California
Berkeley, California

March 8, 1965

Abstract

Design parameters for accelerator vacuum systems are studied with reference to the requirements which appear in modern strong-focusing machines. The two major problems considered are restrictions in both pumpdown time and system base pressure created by trends toward very small apertures.

Basic kinetic equations are used in a method of estimating performance. Assuming a time-dependent outgassing rate from vacuum chamber walls, equations are offered for predicting progression of evacuation and base pressure distribution throughout the system.

Results from small-scale experimental systems are reported and compared with predicted performance. Influence of various pumping systems on prediction is discussed, and design recommendations are offered.

Introduction

Where the alternating gradient principle is used (presently in synchrotrons and storage rings), economy generally dictates that apertures be as small as possible. This consideration of economy becomes even more important with increasing machine size, and to show order of magnitude, we have made informal cost estimates for special cases which indicate that the incremental cost of 1 inch of vertical aperture per mile of diameter is about $20 million. Therefore the trend in accelerator vacuum chamber design is towards increasing ratio of length in beam direction to characteristic cross-sectional dimension. As a result the vacuum chamber is becoming extremely conductance limited and therefore new techniques may have to be applied in estimating a proper pumping system.

Previously vacuum chambers were of such a shape that the free molecular conductance between any two points within the chamber for all practical purposes was considered infinite, and pressure gradients were ignored. Consequently the required pumping speed was estimated as the ratio between total system outgassing rate and the desired operating pressure.

In a conductance-limited vacuum chamber, on the other hand, considerable pressure gradients may exist, which may delay the turn-on time of the high-vacuum pumps and significantly degrade

---

*Work done under the auspices of the U. S. Atomic Energy Commission.

the particle beam. Consequently, for design purposes it becomes necessary to find the effect of chamber dimensions as well as pumping speed on pressure distribution throughout the system.

Pressure gradients for special applications have been calculated.[1,2] It is the purpose in this paper to present a more general method for estimating pressures in conductance limited vacuum chambers and to verify their accuracy experimentally.

System Characteristics

The vacuum chamber in a synchrotron is mostly a ring-shaped tube of constant cross section. The pumping system consists of several vacuum pumps each connected to the ring through a long manifold. Most economically these pump-manifold combinations are made identical and distributed at equal intervals. The number of pumps is generally a plain fraction of the number of magnets.

For this investigation the vacuum system is divided into a number of identical units, each consisting of a pump-manifold combination and an equal length of vacuum chamber on either side extending half way to the neighboring pumps. We assume outgassing from the vacuum chamber wall to be the only significant gas load, with no net gas flow midway between pumps; each unit may then be treated as an independent vacuum system. In the following only one half of a unit is considered.

Theoretical Derivation of Pressure During Molecular Flow

Figure 1 is a sketch of such simplified vacuum system. A tube of length L, cross-sectional periphery H, and cross-sectional area A is at one end connected to a vacuum pump through a manifold. At the connection to the vacuum chamber, pumping speed is S and the aperture is A.

At the ultimate pressure a uniform outgassing, of q per unit area and unit time is assumed to exist. Pressures are $P(0)$ at the entrance to the manifold, $P(L)$ at the other end of the tube, and $P(x)$ at distance x from manifold.

Using the basic equation $P = Q/S$ where Q is the total outgassing rate, $S(x)$ is pumping speed at x, and u is an integration variable, we can write

$$P(x) = \int_0^x \frac{qH\,du}{S(u)} + \frac{qH(L-x)}{S(x)} . \qquad (1)$$

An expression for finding the system pumping

speed $S(u)$ is

$$S(u) = \frac{1}{4} \bar{v} A \cdot W(u) = S_{max} \cdot W(u), \quad (2)$$

where $\bar{v}$ is the mean average molecular velocity and $W(u)$ is the combined probability that a particle which passes point U towards the pump will proceed through the tube section of length u, and be captured by the pump, without being thrown back past point U. S_{max} is the maximum attainable pumping speed through an aperture A.

The probability $W_1(u)$ of transfer through a tube of length u has been calculated for a circular tube by Clausing,[3] and calculation has been experimentally verified by Milleron and Levenson.[4] An approximate expression for tube of arbitrary but constant cross section developed by Dushman[5] is

$$W_1(u) = \frac{1}{1+\frac{3}{16}\frac{H}{A}u} \quad . \quad (3)$$

The probability W_2 of capture by the pump is

$$W_2 = \frac{S}{S_{max}} = \epsilon , \quad (4)$$

where ϵ is the efficiency of pumping through aperture A. If pump aperture is A_0, smaller than tube aperture A, then the probability W_2 is reduced by the ratio A_0/A.

Oatley[6] has found that for equipment connected in series their combined probability for pumping may be found with good approximation by use of

$$W(u) = \frac{W_1(u) \cdot W_2}{W_1(u) + W_2 - W_1(u) \cdot W_2} \quad (5)$$

Substituting Eqs. (3) and (4) in (5), and inserting the resulting expression for $W(u)$ in Eq. (2), we find

$$S(u) = \frac{1}{4} \bar{v} A \left(\frac{1}{\epsilon} + \frac{3}{16}\frac{H}{A}u \right)^{-1} \quad (6)$$

and similarly, for $S(x)$

$$S(x) = \frac{1}{4} \bar{v} A \left(\frac{1}{\epsilon} + \frac{3}{16}\frac{H}{A}x \right)^{-1} \quad (7)$$

The above method for calculating system pumping speed is often much more accurate than the more commonly used electrical analogy.

Substitution of Eqs. (6) and (7) in Eq. (1) and integration result in the explicit expression

$$P(x) = \frac{qH}{\frac{1}{4}\bar{v}A} \left(-\frac{3}{32}\frac{H}{A}x^2 + \frac{3}{16}\frac{H}{A}Lx + \frac{L}{\epsilon} \right) . \quad (8)$$

Equation (8) shows that pressure in the vacuum chamber increases with x according to a parabola with its apex at $x = L$. Pressures $P(L)$ and $P(0)$ and pressure difference ΔP are

$$P(L) = \frac{qH}{\frac{1}{4}\bar{v}A} \left(\frac{3}{32}\frac{H}{A}L^2 + \frac{L}{\epsilon} \right) , \quad (9)$$

$$P(0) = \frac{qH}{\frac{1}{4}\bar{v}A} \cdot \frac{L}{\epsilon} = \frac{qHL}{S} , \quad (10)$$

$$\Delta P = P(L) - P(0) = \frac{3}{8}\frac{q}{\bar{v}} \left(\frac{HL}{A} \right)^2 . \quad (11)$$

At the ultimate pressure where q is constant, Eq. (11) shows that ΔP is independent of pumping speed.

The average pressure $\bar{P}$ for the whole tube is found by integrating $P(x)$ and dividing by L,

$$\bar{P} = \frac{1}{L} \int_0^L P(x) = \frac{qH}{\frac{1}{4}\bar{v}A} \left(\frac{1}{16}\frac{H}{A}L^2 + \frac{L}{\epsilon} \right) . \quad (12)$$

Graphic Estimate of Pressures

Total outgassing of the vacuum chamber is $Q = qHL$. The smallest pressure P_{min} attainable with outgassing Q and pumping aperture A would be $P_{min} = Q/S_{max}$. We can now, from Eq. (12), derive ratio $a = \bar{P}/P_{min}$.

$$a = \frac{1}{16}\frac{HL}{A} + \frac{1}{\epsilon} . \quad (13)$$

For a cylindrical tube with inside radius a, Eq. (13) will be

$$a_c = \frac{1}{8}\frac{L}{a} + \frac{1}{\epsilon} . \quad (14)$$

In a similar way, for an elliptical tube with ratio of semiaxes $\delta = b/a$ and circumference $H = 2\pi [(a^2 + b^2)/2]^{1/2}$, Eq. (13) becomes

$$a_e = \frac{1}{8}\frac{L}{a} \sqrt{\frac{1}{2}(1+(\frac{1}{\delta})^2)} + \frac{1}{\epsilon} . \quad (15)$$

Figure 2 shows a_c and a_e as a function of L/a for various values of δ and ϵ.

Graphical calculations may also be done by use of Fig. 3, which is based on Eqs. (10) and (11). The technique of estimating $P(L)$ and $\bar{P}$ is in this way simplified to

(a) calculation of $P(0)$ according to the usual equation $P = Q/S$ after selection of vacuum chamber dimensions and pumping speed of vacuum pump,

(b) finding of ΔP from Figure 3 after estimating outgassing q and ratio ϵ,

(c) adding of results from (a) and (b) according to

$$P(L) = P(0) + \Delta P, \quad (16)$$

$$\bar{P} = P(0) + \frac{2}{3}\Delta P. \quad (17)$$

It has been shown that outgassing q decreases with time. This means that pressure is a function of both distance x and time t. However, as long as q is reasonably uniform throughout the vacuum chamber the above equations can be corrected to include this by substituting q with its time-dependent function.

Evacuation in the Viscous Pressure Range

Like the high-vacuum pumps, roughing pumps will presumably be distributed along the vacuum chamber at equal but perhaps larger intervals. Therefore the physical layout for estimating pressures in the viscous range is the same

as that used for molecular flow (see Fig. 1). However, as the kinetic laws for viscous flow are not the same as for molecular flow, it will be necessary to change the derivation.

The pressure drop in a tube is commonly expressed as $\Delta P = Q/C$, where Q is gas flow rate and C is conductance of the tube. This equation may be used on a small element dx of the tube,

$$d P(x) = Q(x)/C_{dx} \qquad (18)$$

It is assumed that the gas flow rate $Q(x)$ varies linearly with distance x, indicated by

$$Q(x) = S_0 P_0 (1 - \frac{x}{L}) \qquad (19)$$

where S_0 is speed, P_0 pressure at roughing pump and L is the length of the tube. This is true for steady state, and a good approximation after the first few minutes of roughing.

Dushman[7] has given an equation for estimating the conductance (in liters/sec) of an elliptical tube with semiaxes a, b, and L in cm. If $\bar{P}$ is average pressure in torr, we have, for an element of length dx,

$$C_{dx} = 5.68 \cdot 10^3 \; \frac{\bar{P}}{dx} \; (\frac{a^3 b^3}{a^2+b^2}) . \qquad (20)$$

Substitution of Eqs. (19) and (20) in (18), where $\bar{P} = P(x)$ in the element dx, gives

$$P(x) d P(x) = \frac{S_0 P_0}{5.68 \cdot 10^3} (1 - \frac{x}{L}) \frac{a^2+b^2}{a^3 b^3} dx . \qquad (21)$$

Integration between the limits 0 and L for both sides of Eq. (21) gives the explicit expression for P_L,

$$P_L = \left[\frac{S_0 P_0}{5.68 \cdot 10^3} \; \frac{a^2+b^2}{a^3 b^3} L + P_0^2 \right]^{1/2} . \qquad (22)$$

The pressure estimate may now be performed by first calculating P_0 from the usual equation

$$t = K \frac{V}{S_0} \ell n \frac{P_{atm}}{P_0} , \qquad (23)$$

where P_{atm} is atmospheric pressure, V is total volume of vacuum chamber, and K is an empirical constant. Eq. (22) will then give P_L for any P_0.

Experimental Setup

Two experimental vacuum systems were built in order to evaluate the equations developed in the previous sections; one for testing in the molecular range, and one for the viscous range.

A sketch of the former system is shown in Figure 4. The vacuum chamber was a stainless steel tube of 7.3 cm i.d. and 900 cm long. At one end of the chamber was a small pump manifold with two high-vacuum pumps, at the other end a flange with a leak valve for gauge calibration and pumping-speed measurement. Four ionization

gauges of nude Bayard-Alpert Type (RCA-DEV. NO. J1981) were mounted along the tube.

Gauge No. 1 was placed about 10 cm from the pumping manifold. Gauges Nos. 2, 3, and 4 were placed along the tube respectively 219, 438, and 876 cm from gauge No. 1. One of the two high-vacuum pumps was a 4-in. diffusion pump (NRC Model HS4-750) provided with cold cap, water baffle, liquid nitrogen trap, and pneumatically controlled gate valve. The other pump was a Varian 15-liter/sec Standard VacIon*Pump.

The Varian pump was provided with a Con-Flat*flange, and all other tube flanges had aluminum foil seals. [8] The high-vacuum side above the trap was exposed only to three elastomer seals (viton), all in the gate valve. Fore vacuum and roughing pump was a liquid nitrogen trapped mechanical pump (Kinney Model KC-5). No components (except VacIon Pump) were baked. The vacuum chamber was chemically cleaned by circulation of hot trichloroethylene, subsequent rinsing with acetone, and final drying with cylinder nitrogen blast.

The second vacuum system for measurement in the viscous pressure range was a stainless steel tube of 0.40 in. i.d. and 10 ft long, provided with a thermocouple gauge at either end, and a small mechanical pump (Welch Duoseal 1400B) at one end.

Test Procedure and Results

The high-vacuum system was operated about 1 month prior to actual testing. During this period of "conditioning", pressures kept decreasing slowly. Finally outgassing settled down at 1 to 2×10^{-10} torr liter/sec. cm^2, and the pressure at the pump reached 5×10^{-8} torr. At this level the system was very temperature-dependent, and 5° C increase in room temperature would increase pressure reading on gauge No. 4 as much as 50%.

Rate-of-rise tests were first performed by turning off pumps. Natural outgassing and a slight leak of dry nitrogen were used as calibration gas. After a few seconds (necessary to establish a uniform pressure in the tube), pressure readings agreed within $\pm 10\%$. Correction charts were plotted to make as close a correlation between gauges as possible.

Pumping speed at gauge No. 1 was then calculated for each individual pump with the equation $S = C [(P_4/P_1) - 1]$, where C is the conductance of the vacuum chamber between gauges No. 4 and No. 1 (4.7 liter/sec), and P_4 and P_1 respective gauge readings. Calculations indicated the constant N_2 speeds of 65 liter/sec for diffusion pump and 12 liters/sec for sputter-ion pump systems. This was well within $\pm 10\%$ of values arrived at from manufacturers' rating and calculated conductances.

---

* Trade names registered by Varian Associates, Palo Alto, Calif.

The system was now left to be pumped in turn by either of the two pumps for extended periods. Meanwhile the pressures were observed. Observations agreed with Eqs. (8), (9), (10), and (11) to within 5 to 10%. Both parabolic distribution and independence between ultimate pressure drop and pumping speed were found.

The system was repreatedly let up to dry nitrogen and subsequently evacuated to the base pressure by either of the two pumps in turn. Pressures P_1 and P_4 were recorded. In Fig. 5 outgassing q calculated from Eq. (10) is shown for typical evacuations. In Figs. 6 and 7 respectively recorded pressures are shown for evacuation with sputter-ion and diffusion pump. Broken lines show pressures $P(L)$ calculated according to Eqs. (11) and (16), with q calculated from Eq. (10). For both evacuations, t = 0 was defined as the moment when the pneumatically controlled valve to the diffusion pump was opened. In evacuation with the sputter-ion pump, the valve was closed again after reaching 10^{-5} torr, where the sputter-ion pump could easily handle the gas load.

The vacuum system for evacuation in the viscous range was also allowed to reach its base pressure. However, this took only a few days. Then the two thermocouple gauges were compared by rate-of-rise method, and readings were found to correspond within ±10% between 10 and 200 mtorr. Pumping speed tests were now run with a leak valve and a displacement flow meter. Pumping speed varied from 0.1 to 0.15 liter/sec in the range from 10 to 200 mtorr. The vacuum system was brought up to dry nitrogen pressure and the relationship between pressures at the pump P_0 and at the far end P_L in subsequent evacuations were recorded. Figure 8 shows plots of a typical run.

Discussion and Conclusions

Figure 6 indicates a very close agreement between calculated and experimental values of pressure; in Fig. 7 they do not agree so well until the base pressure is reached.

In the authors' opinion the disagreement is in part due to the difference in pumping speed. At higher pumping speeds the sitting time of nitrogen particles on the vacuum chamber walls become significant and outgassing decreases toward the pump aperture. At sufficiently lower speeds this sitting time can be neglected and net outgassing is more nearly uniform throughout the full length of the vacuum chamber.

Figure 5 also shows that outgassing based on pressure at $P(0)$ is quite different for the two pumping speeds. However, with $P(L)$ used as a basis for the calculations, outgassing curves become almost identical. Therefore, the latter value should be used for estimating pressures. An approximate value for outgassing of nitrogen as a function of time according to Fig. 5 seems to

be
$$q = 10^{-9}/t \qquad\qquad \text{torr liter/sec} \cdot \text{cm}^2.$$

Towards the end of evacuation this function changes because other gases become predominant. Each time the system was let up to dry nitrogen no air was allowed to enter. In case of repair and maintenance it is impossible to prevent some air from entering. This will affect outgassing and tests should be run on other gases (such as oxygen and water vapor) to investigate their relative influence.

It is worth noting that, although pumping speed does not have a pronounced effect on base pressure (because of the conductance limitation), it can have an appreciable effect on the time rate of change of pressures during the beginning of evacuation. Especially where sputter-ion pumps are chosen, it is recommended to select a size with some speed to spare. Otherwise as the pump gets older evacuation time may become excessive.

Figure 8 indicates quite close agreement between experiments and the viscous flow Eq. (22), in spite of the varying sensitivity and slow time response of the thermocouple gauges. Equation (22) could be extended to show intermediate pressure as a function of distance, but this was beyond the scope of this paper.

Acknowledgment

References

1. Venema, A., and Bandringa, M., Production and Measurement of Ultra-High Vacua, Philips Tech. Rev. Vol. 20, 1958/59, No. 6, 145-176.

2. Regenstreif, E., The CERN Proton Synchrotron, 3d part, CERN Report 62-3, 1962.

3. Clausing, P., Ann Physik Vol. 12, p. 961 (1932).

4. Davis, D. H., Levenson, L. L., and Milleron, N., Theoretical and Experimental Studies of Molecular Flow through Short Ducts, Lawrence Radiation Laboratory Report, UCRL-5972, July 1960.

5. Dushman, Saul., and Lafferty, J. M., Scientific Foundations of Vacuum Technique, (John Wiley & Sons, Inc., New York 1962), p. 97.

6. Oatley, C. W., Brit. J. Appl. Phys. Vol. 8, (Jan. 1957) pp. 15-19.

7. Dushman, Saul op. cit., 87.

8. Batzer, T. H., and Ryan, J. F., Some New Techniques in Ultra-High Vacuum, Transactions of the Tenth National Vacuum Symposium, 1963 (The Macmillan Co., New York, 1964).
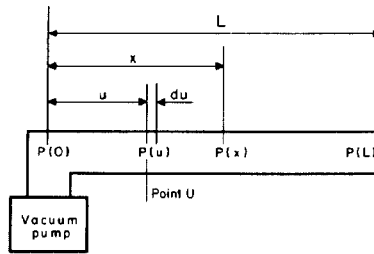
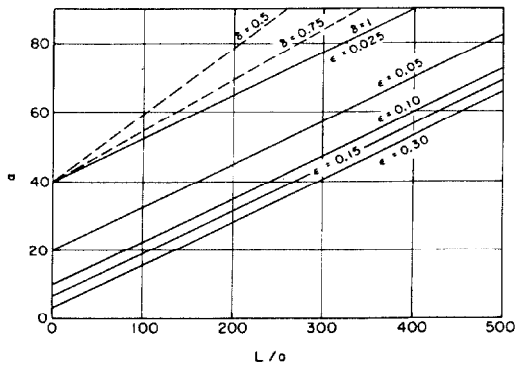Fig. 1. Schematic "half unit"
vacuum system.

Fig. 2. a = P/P$_{min}$ as a function of ratio L/a
for various values of pumping efficiency ϵ and
elliptical flatness δ = b/a. Solid lines show
a for cylindrical tube. Broken lines δ = 0.75
and 0.5 are shown for ϵ = 0.025 only. Various
δ lines for constant ϵ intersect at L/a=0, and
δ lines for various ϵ but equal δ are parallel.
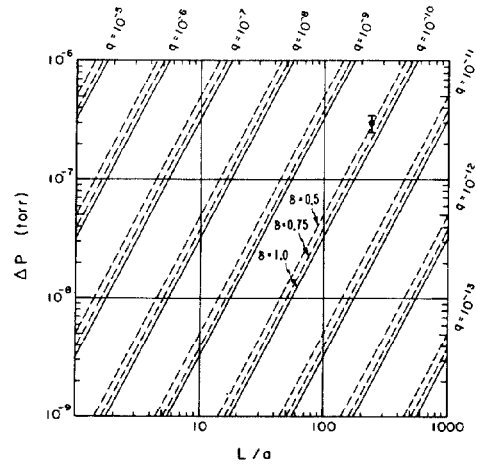
Fig. 3. Pressure gradient ΔP over tube length
L as a function of ratio L/a. Constant outgassing
lines are shown for cylindrical tube   (δ = 1)
and elliptical tubes (δ = 0.75 and 0.5). Unit
of q is torr liters/sec cm^2. ΔP for experimental
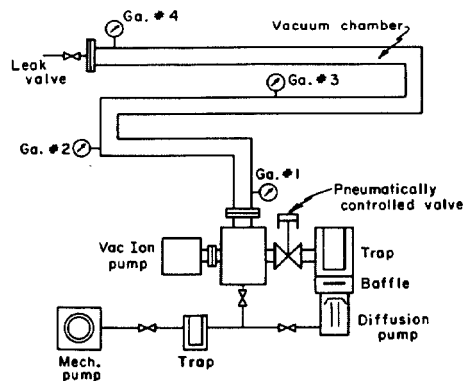system (δ =1, L/a = 240) is shown at ultimate
pressure.

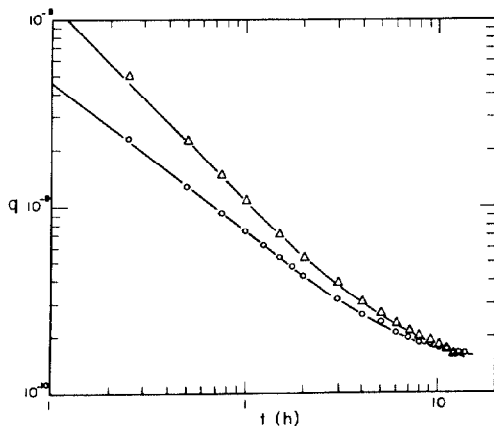Fig. 4. Experimental vacuum system.

Fig. 5. Outgassing (torr liters/sec cm^2) of vacuum chamber walls as a function of time t during evacuation; calculated from Eq. (10)
△ Evacuation with sputter-ion pump (12 liter/sec)
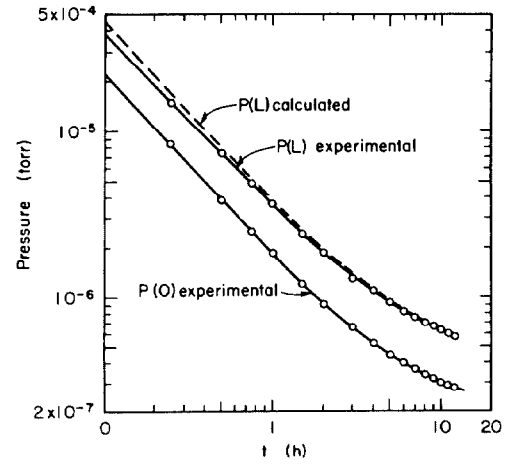◎ Evacuation with diffusion pump (65 liter/sec).

Fig. 6. Pressure p(0) and P(L) at extreme ends of tube as a function of time t during evacuation with sputter-ion pump (12 liters/sec). Theoretical values calculated from Eqs. (9) and (10).
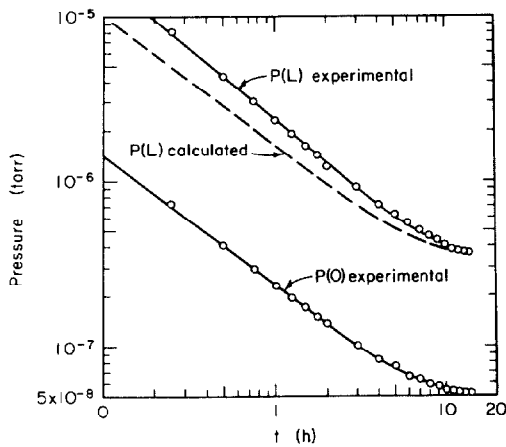

Fig. 7. Pressure P(0) and P(L) at extreme ends of tube as a function of time t during evacuation with diffusion pump (65 liters/sec). Theoretical values calculated from Eqs. (9) and (10).
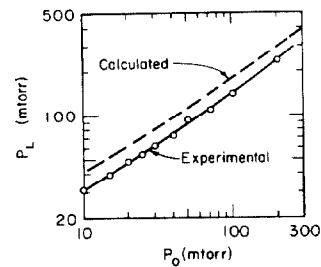

Fig. 8. Pressure P_I as a function of P_0 for tube of length L. Theoretical values calculated from Eq. (27).